

ChemComm

Accepted Manuscript



This is an *Accepted Manuscript*, which has been through the Royal Society of Chemistry peer review process and has been accepted for publication.

Accepted Manuscripts are published online shortly after acceptance, before technical editing, formatting and proof reading. Using this free service, authors can make their results available to the community, in citable form, before we publish the edited article. We will replace this *Accepted Manuscript* with the edited and formatted *Advance Article* as soon as it is available.

You can find more information about *Accepted Manuscripts* in the [Information for Authors](#).

Please note that technical editing may introduce minor changes to the text and/or graphics, which may alter content. The journal's standard [Terms & Conditions](#) and the [Ethical guidelines](#) still apply. In no event shall the Royal Society of Chemistry be held responsible for any errors or omissions in this *Accepted Manuscript* or any consequences arising from the use of any information it contains.

Cite this: DOI: 10.1039/c0xx00000x

www.rsc.org/xxxxxx

ARTICLE TYPE

Porosity control in mesoporous polymers using CO₂-swollen block copolymer micelles as templates and its use as catalyst support

Li Peng, Jianling Zhang*, Shuliang Yang, Buxing Han, Xinxin Sang, Chengcheng Liu and Guanying Yang

Received (in XXX, XXX) Xth XXXXXXXXX 20XX, Accepted Xth XXXXXXXXX 20XX

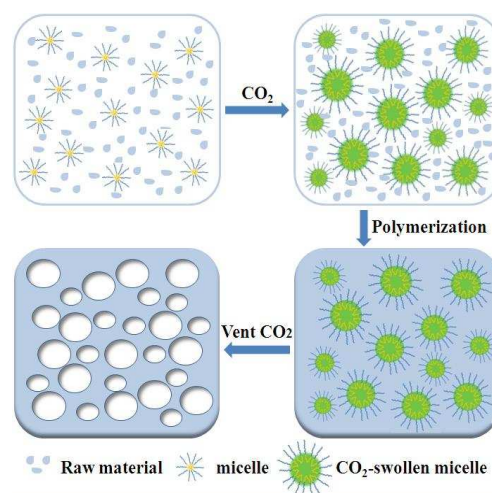
DOI: 10.1039/b000000x

The mesoporous polymers with tunable large mesopores and thin mesopore walls were synthesized through a CO₂-swollen micelle templating route. The mesopore size and porosity properties of the polymers can be easily modulated by adjusting CO₂ pressure. The as-synthesized mesocellular polymers are excellent candidate support for preparing heterogeneous catalysts.

Mesoporous polymers (with pore size range of 2-50 nm) have received an increased research interest because of their potential to combine both properties of mesoporous materials and polymers.¹ They have found wide applications in catalysis,² gas storage and separation,³ templates for structure replication,⁴ electrode materials,⁵ drug release,⁶ etc. Direct templating,⁷ block copolymer self-assembly,⁸ and direct synthesis⁹ methodologies are commonly used to prepare mesoporous polymers. In particular, the self-assembly of block copolymers (BCPs) as pore templates has been developed as one of the best strategies for preparing mesoporous polymers.¹⁰ The mesopore sizes of the porous polymers fabricated by BCP templates are generally quite small and fall into the range of 3-10 nm,¹¹ which restricts their wide applications. To enlarge the mesopore diameter, the swelling agents or pore expanders (e.g. 1,3,5-trimethylbenzene and tributylphosphate) were introduced into the structure directing template.¹² However, the uptake of commonly used linear aliphatic hydrocarbons (e.g. liquid alkanes) in micelles was rather small, resulting in the restricted size tailoring of porous materials.¹³ Besides, the involvement of solid or liquid additives may inevitably pollute the products and complicate the post treatment. To explore the facile surfactant-assembly templating strategies for preparing large-pore mesoporous polymers and pore size tailoring is very interesting, but continues to be a great challenge.

Herein, we propose a gas-tailored assembly of block copolymers templating route for synthesizing large-pore mesoporous polymer. As shown in Scheme 1, the Pluronic (ethylene oxide/propylene oxide triblock copolymers) micelles can be well expanded by the dissolution of gaseous CO₂. The polymerization proceeds in bulk water phase, during which the CO₂-swollen micelles act as the mesopore template. The mesoporous polymers are formed after polymerization and

removing CO₂, solvent and BCP. This route excels the conventional swelling technique (using solid or liquid as swelling agents) mainly from the following aspects. First, due to the hydrophobic and small molecule nature, CO₂ can be well solubilized in the micelles and the solubility can be controlled by pressure; therefore, the mesopore size of the polymers can be tuned in a large range by controlling operation pressure. Second, CO₂ can be easily removed by depressurization, thus no contamination to the product is involved and the post-processing is simple. In addition, CO₂ is nontoxic, inexpensive, and can be easily recaptured and recycled after use. This strategy is different from the CO₂-in-liquid emulsion templating route, which utilized the micron sized CO₂ droplets as templates for macropore formation.¹⁴ By the CO₂-tailored assembly of block copolymers templating route, the highly mesoporous polymers with tunable mesopore size (14-22 nm) were obtained. The as-synthesized polyacrylamide (PAM) was used as a support for Pd nanoparticles and the Pd/PAM composite showed high catalytic activity and selectivity for the hydrogenation of phenylacetylene to yield styrene.



Scheme 1. Schematic illustration for the formation of mesoporous polymer with CO₂-tailored assembly of block copolymers.

Polyacrylamide is one of the most extensively explored polymer for its various use.¹⁴ Herein we synthesized porous PAM at 60 °C, using F127 (EO₁₀₆PO₇₀EO₁₀₆) to form micelles. First of all, the PAM was synthesized in F127 aqueous solution in the absence of CO₂. The product appeared as irregular agglomerates (Fig. S1, ESI†). The N₂ adsorption-desorption isotherms (Fig. S2, ESI†) reveal that the BET (Brunauer, Emmett, and Teller) surface area and total pore volume of the PAM are very low, i.e., 20.3 m²g⁻¹ and 0.108 cm³g⁻¹, respectively. The mesopore size centers at 3.5 nm, which is comparable to the mesopore size of the silica synthesized by F127 micelle template.¹⁵

The PAMs were synthesized in the CO₂-present 10 wt% F127 aqueous solution at different pressures. As an example, Fig. 1 shows the SEM images of the PAM synthesized at 4.5 MPa. The PAM is highly porous with a mesocellular structure. The mesopore size is around 10-30 nm, much larger than the mesopores of the PAM synthesized without CO₂. The wall of the mesopore is ~5 nm. The TEM image further proved that the polymer adopted a mesoporous structure (Fig. S3, ESI†). The FT-IR spectra indicate the successful formation of PAM and the monomers are polymerized completely (Fig. S4, ESI†). Thermogravimetric (TG) analysis under N₂ atmosphere revealed that the PAM keeps stable up to 260 °C (Fig. S5, ESI†).

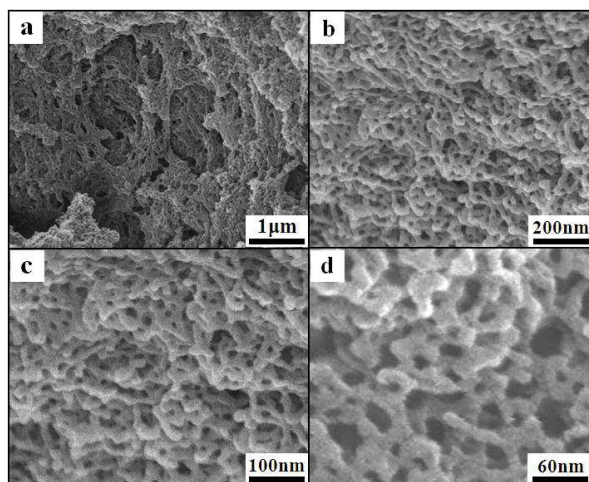


Fig. 1 SEM images of the PAM synthesized in the CO₂-present 10 wt% F127 aqueous solution at pressure of 4.8 MPa.

The mesoporosity of the PAM was determined by N₂ adsorption-desorption method and the results are shown in Fig. 2. It exhibits the mode of type IV, which is related to mesoporous materials. The BET surface area (S_{BET}) and total pore volume (V_t) is 143.6 m²g⁻¹ and 0.718 cm³g⁻¹, respectively. In comparison with the PAM synthesized without CO₂, evidently, the porosity of the PAM is greatly increased by the addition of CO₂. Also, the mesopore volume of the as-synthesized PAM is higher than those of the reported mesoporous polymer (<0.6 cm³g⁻¹).¹⁶ The mesopore size distribution curve, calculated from Barrett-Joyner-Halenda analysis, is shown in the inset of Fig. 2. It centers at around 17 nm, consistent with that measured from the SEM

images shown in Fig. 1. The result proves that CO₂ is capable of enlarging the mesopores of the PAM templated by F127 micelles.

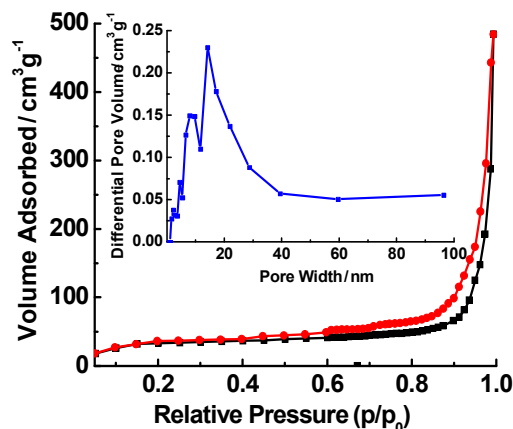


Fig. 2 N₂ adsorption-desorption isotherms of the PAM synthesized in the CO₂-present 10 wt% F127 aqueous solution at pressure of 4.8 MPa. The inset shows the mesopore size distribution curve.

The PAMs were synthesized at different CO₂ pressures, while other experimental conditions were the same with those above. The results show that all the PAMs present mesocellular structures (see SEM images and N₂ adsorption-desorption isotherm results in Fig. S6 and Fig. S7, ESI†). Table 1 lists the mesoporosity properties of the PAMs synthesized at different pressures (No. 2-4). The mesopore enlarges with the increasing pressure, i.e. from 13.8 to 22.0 nm as the pressure is enhanced from 2.5 to 6.9 MPa. It can be attributed to the enlarged F127 micelles at higher pressures, by taking account of the templating effects of micelles on the mesopore formation.¹⁷ The BET surface area and mesopore volume increase as the pressure is enhanced (i.e. with the increased mesopore size), which is very interesting because generally the BET surface area of mesoporous materials decreases with the enlarged mesopores. It is known that apart from dissolving inside micelles, CO₂ can be solubilized in bulk water and the amount of CO₂ solubilized in bulk phase is increased with pressure.¹⁸ Therefore, the PAM synthesized at higher pressure is more porous after releasing CO₂. The above analysis proves that CO₂ is efficient in tuning the mesopore properties of the PAMs through the control of pressure.

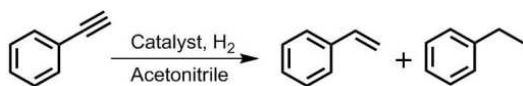
Table 1 The mesopore diameter (D_{meso}), BET surface area (S_{BET}) and mesopore volume (V_t) of the PAMs synthesized in the CO₂-present F127 aqueous solution at different pressures and surfactant concentrations.

No	Pressure/MPa	[F127]/wt%	D_{meso} /nm	S_{BET} /m ² g ⁻¹	V_t /cm ³ g ⁻¹
1	CO ₂ -free	10	3.5	20.3	0.108
2	2.5	10	13.8	105.5	0.455
3	4.8	10	17.0	143.6	0.718
4	6.9	10	22.0	88.8	0.312
5	4.8	2	16.5	60.6	0.169
6	4.8	6	17.2	79.6	0.281

The effect of surfactant concentration on the properties of the PAMs synthesized in the CO₂-present F127 aqueous solution was investigated. The CO₂ pressure was fixed at 4.8 MPa. As the surfactant concentrations were 2.0 and 6.0 wt%, the mesocellular PAMs were also obtained (see SEM images and N₂ adsorption-desorption results in Fig. S8 and Fig. S9, ESI†). The porosities of the two PAMs determined by N₂ adsorption-desorption method are listed in Table 1 (No. 5 and 6). The mesopore sizes of the PAMs synthesized at different surfactant concentrations are nearly identical (~17 nm, No. 3, 5, 6). It can be explained by the fact that the size of the F127 micelles changes little in the experimental surfactant concentration range at the same pressure.¹⁹ However, S_{BET} and V_t drop remarkably as the surfactant concentration is decreased. It further proves the templating effect of the micelles to the mesopore formation, because less micelles are formed at lower surfactant concentrations.

The interconnected nature of the large mesopores makes the as-synthesized polymer promising candidate of catalyst support. The selective hydrogenation of alkynes to alkenes is of great significance in fine chemical industries.²⁰ To facilitate the selectivity towards the desired alkene, generally, the additive of N-bases,²¹ modification of Pd-catalysts by the metals like Pb, Zn,²² utilization of N-group functionalized polymers as Pd support²³ are needed. Here we utilized the as-synthesized unfunctionalized PAM as a support for monometallic Pd catalyst under a non-base condition. The TEM and XRD results confirm that the crystalline Pd nanoparticles in size of ~2 nm are highly dispersed on PAM (Fig. S10 and Fig. S11, ESI†). The Pd loading content was determined to be 1.30 wt% by ICP-AES analysis. The catalytic performance of Pd/PAM composite for the selective hydrogenation of phenylacetylene was tested. As shown in Table 2, 52.1% phenylacetylene could convert within 1 hour with 99.9% selectivity to styrene (Entry 1). With the increasing reaction time, the conversion is increased, while the selectivity drops (Entries 2-5). As the reaction time is 5 hours, phenylacetylene could almost completely convert with 74.5% selectivity to styrene (Entry 5).

Table 2 Hydrogenation of phenylacetylene.



Entry	Time/hour	Conversion/%	Selectivity/%	TOF/h ⁻¹ [a]
1 ^[b]	1	52.1	99.9	1293
2 ^[b]	3	75.6	92.5	626
3 ^[b]	4	91.1	90.1	566
4 ^[b]	4.5	96.5	80.6	532
5 ^[b]	5	99.8	74.5	496
6 ^[c]	5	99.7	75.8	495
7 ^[d]	5	99.8	75.6	497
8 ^[e]	5	96.6	80.2	480
9 ^[f]	1	80.5	8.2	520
10 ^[g]	2	99.8	0	323
11 ^[g]	1	11	89	527

[a]: TOF defined as mmol(product) × (mmol(Pd) × h)⁻¹. [b]: The Pd/PAM catalyst synthesized in this work, reaction condition for Entry 1-8: 0.366 μmol of Pd, phenylacetylene (100 μL, 0.91 mmol) in 2.0 mL acetonitrile using the 1,3,5-trimethylbenzene as the internal standard, 1 atm H₂, 30 °C. [c], [d], [e]: The Pd/PAM was reused for the second, third and fourth runs. [f]: The commercial Pd/C catalyst (3mg, Pd: 5 wt%). [g]: The Pd/bipyridine-functionalized PLA catalyst reported in Ref. 24, Pd (0.834 μmol), phenylacetylene (4 mmol), THF (10 mL), p(H₂) (3 bar), T (25 °C).

The reusability of Pd/PAM for the selective hydrogenation of phenylacetylene was investigated under identical conditions to those of Entry 5. After reaction for 5 hours, the catalyst was recovered by centrifugation, washing with CH₃CN and drying, and then the solid was reused for a consecutive run. As listed in Table 2, the catalyst shows no drop of catalytic activity after three runs (Entry 7). There is a little decrease of conversion for the fourth use (96.6%), which may be due to the loss of catalyst during recovery and washing process, and the selectivity for styrene still keeps unreduced (Entry 8). The TEM image of the Pd/PAM catalyst after reused for four runs shows no particle or crystallite aggregation and the mesoporous structure of the PAM was well preserved (Fig. S12, ESI†). No major difference was observed for the XRD patterns of the fresh Pd/PAM and that after reused for three runs (Fig. S13, ESI†).

For comparison, the catalytic performance of commercial Pd/C composite for the selective hydrogenation of phenylacetylene was tested at the experimental conditions the same as above. Phenylacetylene was completely converted into ethylbenzene in 2 hours, showing absolutely no selectivity to styrene (Entry 10). Besides, the catalytic performance of the as-synthesized Pd/PAM for the selective hydrogenation of phenylacetylene to styrene is compared with that of the Pd/polymer catalysts. As shown in Table 2, the TOF value and selectivity of the Pd/PAM are much higher than the reported catalyst Pd on bipyridine-functionalized poly(lactic acid) (PLA)-based stereocomplexes (Entry 11).²⁴ The high catalytic activity of the as-synthesized Pd/PAM can be ascribed to: 1) XPS spectra of the Pd/PAM (Fig. S14, ESI†) shows that the nitrogen in the amino group of PAM participated in the bonding of Pd, which modified the Pd active centers and thus resulted in stronger adsorption of alkyne substrate to Pd active centers than alkene;²⁵ 2) the highly dispersed small Pd nanoparticles (~2 nm) could increase the density of catalytic active sites;²⁶ 3) the interconnected nature of the large mesopores of support PAM are favourable to the diffusion of substrate and product.²⁷

In summary, the highly porous mesocellular PAMs were synthesized through a CO₂-swollen micelle templating route proposed in this work. The mesopore size of the PAMs can be modulated by adjusting CO₂ pressure. The as-synthesized mesocellular PAMs are excellent support for preparing heterogeneous catalysts. By taking advantages of interconnected nature of the mesopores and high porosity, these mesocellular PAMs have potential applications in catalysis, gas separation, and controlled drug release. The CO₂-tailored BCP self-assemblies can be applied to the synthesis of different kinds of mesoporous polymers.

The authors are grateful to the National Natural Science Foundation of China (21173238, 21133009, U1232203, 21021003), Chinese Academy of Sciences (KJCX2.YW.H16).

Notes and references

Beijing National Laboratory for Molecular Sciences, CAS Key Laboratory of Colloid and Interface and Thermodynamics, Institute of Chemistry Chinese Academy of Sciences, Beijing 100190, P.R.China.

Fax: +86-10-62559373; Tel: +86-10-62562821; E-mail: zhangjl@iccas.ac.cn

† Electronic Supplementary Information (ESI) available: Materials, experimental details, and characterization. See DOI: 10.1039/b000000x/

- 1 a) S. Wan, J. Guo, J. Kim, H. Ihee and D. Jiang, *Angew. Chem. Int. Ed.*, 2009, **48**, 5439–5442; b) Y. H. Xu, S. B. Jin, H. Xu, A. Nagai and D. L. Jiang, *Chem. Soc. Rev.*, 2013, **42**, 8012–8031; c) N. D. Petkovich and A. Stein, *Chem. Soc. Rev.*, 2013, **42**, 3721–3739; d) H. Sai, K. Wee Tan, K. Hur, E. Asenath-Smith, Robert Hovden, Y. Jiang, M. Riccio, D. A. Muller, V. Elser, L. A. Estroff, S. M. Gruner and U. Wiesner, *Science*, 2013, **341**, 530–534.
- 2 a) S. J. Pierre, J. C. Thies, A. Dureault, N. R. Cameron, J. C. M. van Hest, N. Carette, T. Michon and R. Weberskirch, *Adv. Mater.*, 2006, **18**, 1822–1826; b) Y. Zhang, L. Zhao, P. K. Patra and J. Y. Ying, *Adv. Synth. Catal.*, 2008, **350**, 662–666; c) I. Pulko, J. Wall, P. Krajnc and N. R. Cameron, *Chem. Eur. J.*, 2010, **16**, 2350–2354; d) C. E. Chan-Thaw, A. Villa, P. Katekomol, D. Su, A. Thomas and L. Prati, *Nano Lett.*, 2010, **10**, 537–541; e) Y. G. Zhang and S. N. Riduan, *Chem. Soc. Rev.*, 2012, **41**, 2083–2094.
- 3 a) S. S. Han, H. Furukawa, O. M. Yaghi and W. A. Goddard, *J. Am. Chem. Soc.*, 2008, **130**, 11580–11581; b) H. Furukawa and O. M. Yaghi, *J. Am. Chem. Soc.*, 2009, **131**, 8875–8883; c) C. J. Doonan, D. J. Tranchemontagne, T. G. Glover, J. R. Hunt and O. M. Yaghi, *Nat. Chem.*, 2010, **2**, 235–238; d) S. Yuan, B. Dorney, D. White, S. Kirklin, P. Zapol, L. Yu and D. –J. Liu, *Chem. Commun.*, 2010, **46**, 4547–4549; e) R. Dawson, D. J. Adams and A. I. Cooper, *Chem. Sci.*, 2011, **2**, 1173–1177.
- 4 a) W. H. Tseng, C. K. Chen, Y. W. Chiang, R. M. Ho, S. Akasaka and H. Hasegawa, *J. Am. Chem. Soc.*, 2009, **131**, 1356–1357; b) E. J. W. Crossland, M. Kamperman, M. Nedelcu, C. Ducati, U. Wiesner, D. M. Smilgies, G. E. S. Toombes, M. A. Hillmyer, S. Ludwigs, U. Steiner and H. J. Snaith, *Nano Lett.*, 2009, **9**, 2807–2812; c) B. H. Jones and T. P. Lodge, *Chem. Mater.*, 2010, **22**, 1279–1281; d) Y. Wang, C. He, W. Xing, F. Li, L. Tong, Z. Chen, X. Liao and M. Steinhart, *Adv. Mater.*, 2010, **22**, 2068–2072.
- 5 a) R. Liu, S. I. Cho and S. B. Lee, *Nanotechnology*, 2008, **19**, No. 215710; b) Y. Kou, Y. Xu, Z. Guo and D. Jiang, *Angew. Chem. Int. Ed.* 2011, **50**, 8753–8757.
- 6 a) X. Yang, L. Chen, B. Huang, F. Bai and X. Yang, *Polymer* 2009, **50**, 3556–3563; b) M. R. Abidian, D. H. Kim and D. C. Martin, *Adv. Mater.*, 2006, **18**, 405–409.
- 7 a) A. Thomas, F. Goettmann and M. Antonietti, *Chem. Mater.*, 2008, **20**, 738–755; b) A. Stein, F. Li and N. R. Denny, *Chem. Mater.*, 2008, **20**, 649–666.
- 8 a) Y. Wan, Y. F. Shi and D. Y. Zhao, *Chem. Mater.*, 2008, **20**, 932–945; b) Y. Wang and F. Li, *Adv. Mater.*, 2011, **23**, 2134–2148.
- 9 a) C. Weder, *Angew. Chem. Int. Ed.*, 2008, **47**, 448–450; b) A. I. Cooper, *Adv. Mater.*, 2009, **21**, 1291–1295; c) N. B. McKeown and P. M. Budd, *Macromolecules*, 2010, **43**, 5163–5176; d) J. R. Holst and A. I. Cooper, *Adv. Mater.*, 2010, **22**, 5212–5216.
- 10 D. A. Olson, L. Chen and M. A. Hillmyer, *Chem. Mater.*, 2008, **20**, 869–890.
- 11 D. Wu, F. Xu, B. Sun, R. Fu, H. He and K. Matyjaszewski, *Chem. Rev.*, 2012, **112**, 3959–4015.
- 12 a) M. C. Burleigh, M. A. Markowitz, E. M. Wong, J. –S. Lin and B. P. Gaber, *Chem. Mater.*, 2001, **13**, 4411–4412; b) L. Zhao, G. Zhu, D. Zhang, Y. Di, Y. Chen, O. Terasaki and S. Qiu, *J. Phys. Chem. B*, 2005, **109**, 764–768; c) X. F. Zhou, S. Z. Qiao, N. Hao, X. L. Wang, C. Z. Yu, L. Z. Wang, D. Y. Zhao and G. Q. Lu, *Chem. Mater.*, 2007, **19**, 1870–1876; d) L. A. Cao, T. Man and M. Kruk, *Chem. Mater.*, 2009, **21**, 1144–1153.
- 13 a) R. Nagarajan, M. Barry and E. Ruckenstein, *Langmuir*, 1986, **2**, 210–215; b) R. Nagarajan, *Colloid Surface B*, 1999, **16**, 55–72; c) M. Kruk and L. Cao, *Langmuir*, 2007, **23**, 7247–7254.
- 14 a) R. Butler, C. M. Davies and A. I. Cooper, *Adv. Mater.*, 2001, **13**, 1459–1463; b) R. Butler, I. Hopkinson and A. I. Cooper, *J. Am. Chem. Soc.*, 2003, **125**, 14473–14481; c) L. Peng, J. L. Zhang, J. S. Li, B. X. Han, Z. M. Xue and G. Y. Yang, *Angew. Chem. Int. Ed.*, 2013, **52**, 1792–1795.
- 15 T. W. Kim, P. W. Chung and V. S. Y. Lin, *Chem. Mater.*, 2010, **22**, 5093–5104.
- 16 a) J. Weber and L. Bergström, *Langmuir*, 2010, **26**, 10158–10164; b) D. –H. Choi and R. Ryoo, *J. Mater. Chem.*, 2010, **20**, 5544–5550; c) F. Liu, H. Zhang, L. Zhu, Y. Liao, F. Nawaz, X. Meng and F. Xiao, *Adsorption*, 2013, **19**, 39–47.
- 17 J. M. O’Callaghan, H. McNamara, M. P. Copley, J. P. Hanrahan, M. A. Morris, D. C. Steytler, R. K. Heenan and J. D. Holmes, *Langmuir*, 2010, **26**, 7725–7731.
- 18 J. L. Zhang, B. X. Han, Y. J. Zhao, J. S. Li and G. Y. Yang, *Chem. Eur. J.*, 2011, **17**, 4266–4272.
- 19 G. L. Drisko, A. Zelcer, R. A. Caruso, G. J. de and A. A. Soler-Illia, *Microporous Mesoporous Mater.*, 2012, **148**, 137–144.
- 20 R. Chinchilla and C. Nájera, *Chem. Rev.*, 2013, **114**, 1783–1826.
- 21 Červený, V. Kurtc, L. Bronstein, O. Platonova and P. Valetsky, *Appl. Catal. A*, 1999, **176**, 75–81.
- 22 a) P. Kukula and L. Červený, *J. Mol. Catal. A*, 1999, **148**, 245–251; b) Á. Molnár, A. Sárkány and M. Varga, *J. Mol. Catal. A*, 2001, **173**, 185–221.
- 23 A. Drelinkiewicz, A. Knapik, W. Stanuch, J. Sobczak, A. Bukowski and W. Bukowski, *React. Funct. Polym.*, 2008, **68**, 1652–1664.
- 24 G. Petrucci, W. Oberhauser, M. Bartoli, G. Giachi, M. Frediani, E. Passaglia, L. Capozzoli and L. Rosi, *Appl. Catal. A*, 2014, **469**, 132–138.
- 25 Z. –L. Wang, J. –M. Yan, H. –L. Wang, Y. Ping and Q. Jiang, *J. Mater. Chem. A*, 2013, **1**, 12721–12725.
- 26 A. Carné, C. Carbonell, I. Imaz and D. MasPOCH, *Chem. Soc. Rev.*, 2011, **40**, 291–305.
- 27 W. Xuan, C. Zhu, Y. Liu and Y. Cui, *Chem. Soc. Rev.*, 2012, **41**, 1677–1695.